PHYSICAL REVIEW D

PARTICLES AND FIELDS

THIRD SERIES, VOLUME 38, NUMBER 9 1 NOVEMBER 1988

Electroweak studies in e^+e^- collisions: $12 < \sqrt{s} < 46.78$ GeV

B. Adeva,[f] H. Anderhub,[j] S. Ansari,[d] U. Becker,[e] R. Becker-Szendy,[a] J. Berdugo,[f] A. Boehm,[a] M. Bourquin,[i] J. G. Branson,[e,*] J. D. Burger,[e] C. Camps,[a] M. Cerrada,[f] C. C. Chang,[g] Y. H. Chang,[e] H. S. Chen,[g] M. Chen,[e] M. L. Chen,[g] M. Y. Chen,[g] V. Commichau,[a] E. Deffur,[a] K. Deiters,[h] M. Dhina,[e,†] J. Fehlmann,[j] H. S. Fesefeldt,[a] D. Fong,[e,‡] W. Friebel,[h] M. Fukushima,[e] L. Garrido,[f] K. Z. Guo,[g] R. D. Han,[g] K. Hangarter,[j] R. Hausammann,[i] G. Herten,[a,§] U. Herten,[a] H. Hofer,[j] D. Hueser-Teuchert,[a] M. M. Ilyas,[e] W. Krenz,[a] R. Leiste,[h] Q. Z. Li,[j] D. Linnhoeffer,[a] D. Luckey,[e] H. Ma,[c] W. Ma,[g] C. Mana,[f] M. A. Marquina,[f] M. Martinez,[f] J. Mnich,[a] H. Newman,[c] H. Nierobisch,[a] W. D. Nowak,[h] M. Nusbaumer,[i] M. Pohl,[j] R. R. Rau,[b] D. Ren,[j] S. Rodriguez,[f] M. Rohde,[d] J. Rose,[a] J. A. Rubio,[f] H. Rykaczewski,[e] M. Sachwitz,[f] J. Salicio,[f] H. J. Schreiber,[h] U. Schroeder,[a] J. Schug,[a] P. Schulte,[h] H. Stone,[c] H. W. Tang,[g] Samuel C. C. Ting,[e] M. Tonutti,[a] K. L. Tung,[g] D. Twerenbold,[j] G. Viertel,[j] H. Vogt,[h] Z. M. Wang,[g] M. White,[e] H. G. Wu,[d] S. X. Wu,[a] M. F. Wyne,[d] B. Wyslouch,[e] B. X. Yang,[g] B. Zhou,[e,**] and R. Y. Zhu[c]

[a]*III. Physikalisches Institut, Technische Hochschule, D-5100 Aachen, Federal Republic of Germany*

[b]*Brookhaven National Laboratory, Upton, New York 11973*

[c]*California Institute of Technology, Pasadena, California 91125*

[d]*Deutsches Elektronen Synchrotron, D-2000 Hamburg 52, Federal Republic of Germany*

[e]*Laboratory for Nuclear Science, Massachusetts Institute of Technology, Cambridge, Massachusetts 02139*

[f]*Junta de Energia Nuclear, Madrid, Spain*

[g]*Institute of High Energy Physics, Chinese Academy of Science, Beijing, People's Republic of China*

[h]*Institut für Hochenenergiephysik, Akademie der Wissenschaften der Deutschen Demokratischen Republik, DDR-1615, Berlin-Zeuthen, Germany*

[i]*Universite de Geneve, CH-1211 Geneva 23, Switzerland*

[j]*Institut für Hochenenergiephysik, Eidgenossische Technische Hochschule, CH-8093 Zurich, Switzerland*

(The Mark J Collaboration)

(Received 29 April 1988)

The Mark J Collaboration at the DESY e^+e^- collider PETRA presents results on the electroweak reactions $e^+e^-\to\mu^+\mu^-$, $\tau^+\tau^-$, $\mu^+\mu^-\gamma$, and $e^+e^-\mu^+\mu^-$. The c.m. energy range is 12 to 46.78 GeV. In the $\mu^+\mu^-$ and $\tau^+\tau^-$ channels the total cross sections and the forward-backward asymmetries are reported and compared with other experiments. The results are in excellent agreement with the standard model. The weak-neutral-current vector and axial-vector coupling constants are determined. The values for muons and τ's are compatible with universality and with the predictions of the standard model. In the $\mu^+\mu^-\gamma$ channel, all measured distributions, including the forward-backward muon asymmetry, are in excellent agreement with the electroweak theory. Our data on the two-photon process, $e^+e^-\mu^+\mu^-$, agrees with QED to order α^4 over the entire energy range and the Q^2 range from 0.7 to 166 GeV^2.

I. INTRODUCTION

At PETRA, the e^+e^- collider at the DESY Laboratory, the c.m. energy $\sqrt{s}$ covered the range from 12 to 46.78 GeV, a significant fraction of the mass of the Z^0, the weak-neutral-vector boson. In this paper, the Mark J Collaboration presents concluding results for the production channels $e^+e^-\to\mu^+\mu^-$, $\tau^+\tau^-$, $\mu^+\mu^-\gamma$, and $e^+e^-\mu^+\mu^-$, which test the standard electroweak model over this very large energy range.

II. $e^+e^-\to\mu^+\mu^-$

In terms of the standard model of the electroweak theory,[1] the effect of the weak-neutral-current interaction has been observed in the muon- and τ-pair production

channels.[2] Generally the total or differential cross sections have three components (we use $\mu\mu$ generically)

$$\sigma(\mu\mu)=\sigma(\text{QED})+\sigma(\text{int})+\sigma(\text{weak}) . \quad (1)$$

The middle term is the interference between QED and the weak interactions. In the lowest order, the Born approximation, the differential cross section is

$$\frac{d\sigma(\mu\mu)}{d(\cos\theta)}=\frac{\pi\alpha^2}{2s}[R_{\mu\mu}(1+\cos^2\theta)+B_{\mu\mu}\cos\theta] . \quad (2)$$

θ is the total angle between the produced μ^- and the e^- beam. $R_{\mu\mu}$ is the total cross section normalized to the point QED cross section, $\sigma(\text{QED})=4\pi\alpha^2/3s=86.85/s$ nb (s in GeV^2):

$$\begin{aligned} R_{\mu\mu}&=\frac{\sigma(\mu\mu)}{\sigma(\text{QED})} \\ &=1-2g_V^e g_V^\mu \chi \\ &\quad +[(g_V^e)^2+(g_A^e)^2][(g_V^\mu)^2+(g_A^\mu)^2]\chi^2 \end{aligned} \quad (3)$$

and

$$B_{\mu\mu}=-4g_A^e g_A^\mu \chi+8g_V^e g_V^\mu g_A^e g_A^\mu \chi^2 .$$

g_V, g_A are the vector and axial-vector neutral-current coupling constants. In the standard model,

$$\begin{aligned} g_A&=-\tfrac{1}{2} , \\ g_V&=-\tfrac{1}{2}-2Q_f\sin^2\theta_W , \end{aligned} \quad (4)$$

and g_A and g_V are each the same for the three charged leptons (universality). θ_W is the weak mixing angle, defined as

$$\cos\theta_W=\frac{m_{W^\pm}}{m_{Z^0}} . \quad (5)$$

Q_f is the charge of the fermion. The propagator term χ can be written[3]

$$\chi=\frac{1}{4\sin^2\theta_W\cos^2\theta_W}\frac{s}{m_{Z^0}^2-s} . \quad (6)$$

m_W and M_{Z^0} are the masses of the weak charged and neutral bosons, respectively. We have taken the width of the Z^0, $\Gamma_{Z^0}<3$ GeV, and thus the imaginary part of the propagator is small and is neglected.

In the differential cross section Eq. (2), the $\cos\theta$ term dictates that there will be a forward-backward asymmetry. The coefficient $B_{\mu\mu}$ determines the magnitude of the asymmetry:

$$A_{\mu\mu}=\frac{F-B}{F+B}=\frac{3B_{\mu\mu}}{8R_{\mu\mu}}\simeq-\tfrac{3}{2}\chi g_A^e g_A^\mu . \quad (7)$$

We omit writing the second-order term in χ^2 in the second line of Eq. (7). Figure 1 shows the general characteristics of $R_{\mu\mu}$ and $A_{\mu\mu}$ predicted by the model with the parameters

$$\begin{aligned} &\sin^2\theta_W=0.23, \quad m_{Z^0}=91.9 \text{ GeV} , \\ &\Gamma_{Z^0}=3 \text{ GeV} . \end{aligned} \quad (8)$$

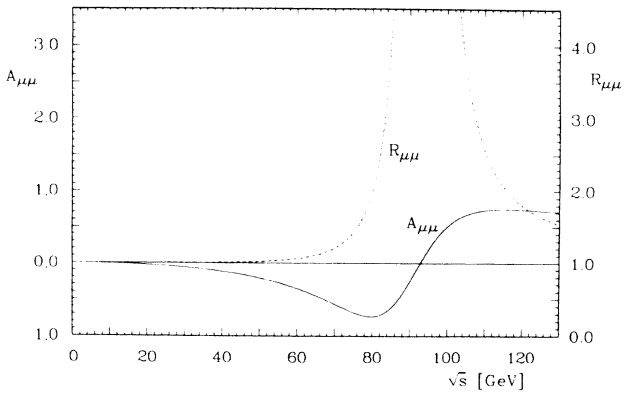

FIG. 1. The standard-model predictions for $R_{\mu\mu}$ and $A_{\mu\mu}$ as a function of $\sqrt{s}$.

The equations and considerations apply equally to $e^+e^-\to\tau^+\tau^-$ in Sec. III.

In the energy region available at PETRA, the total cross section $R_{\mu\mu}$ deviates from the QED point cross section by less than 1%. This arises from the fact that the vector coupling $g_V^e\simeq-0.04$ for the measured value (world averaging) of $\sin^2\theta_w\simeq0.23$. In Eq. (3) the interference term in $R_{\mu\mu}$ is in fact smaller than the weak term. In the asymmetry $A_{\mu\mu}$, the situation is different since it depends upon the axial-vector coupling and $g_A^e g_A^\mu=\frac{1}{4}$ in the standard model. At 35 GeV the expected asymmetry is -9.0% and at 44 GeV -15.7%.

In Eqs. (2)–(7) we have used only Born terms of order α^2: the single-photon- and Z^0-exchange diagrams. For a precise comparison of the electroweak prediction with the measurements, we must take into account radiative processes. Following the usual procedure we correct the measured data for acceptance and radiative effects such that they can be compared to the Born-term electroweak prediction. A Monte Carlo program generates events according to the cross section of order α^3, including all one-loop electroweak radiative diagrams.[4] This program permits the detailed simulation of the acceptance and the resolution of the detector. For a given luminosity we determine from the data $M(\cos\theta)$, the number of events in an interval of $\cos\theta$ accepted by the detector, and satisfying the selection criteria. This number is compared to $M_0(\cos\theta)$, the number of events calculated by the Born-term cross section for the same acceptance and luminosity. The corrected cross section $d\sigma/d(\cos\theta)$ is then calculated from the measured cross section $d\sigma(\text{expt})/d(\cos\theta)$ by

$$\frac{d\sigma}{d(\cos\theta)}=\frac{d\sigma(\text{expt})}{d(\cos\theta)}\frac{M_0(\cos\theta)}{M(\cos\theta)} . \quad (9)$$

In the calculation of the radiative corrections we use the physical parameters α, $m_{W^\pm}$, m_{Z^0} and define $\cos\theta_w$ by Eq. (5). Additional parameters are the masses of leptons and quarks. The masses of the Higgs-scalar particle and the top quark are not known. If the Higgs-boson mass is below 1000 GeV and the top-quark mass is less than 200 GeV, the radiative corrections[5] are very insensitive to the values of these masses. If the top-quark mass

is much larger than 200 GeV, the electroweak radiative corrections change substantially due to the self-energy of the Z^0.

The uncertainty of the radiative corrections, due to the unknown top-quark mass, can be avoided by rewriting the asymmetry using the relation

$$m_{W^\pm}^2 = \frac{\pi\alpha}{\sqrt{2}G_F \sin^2\theta_W} \frac{1}{1-\Delta r_W} , \tag{10}$$

where G_F is accurately measured at low energies using the decay of the muon. Equation (10) has a correction term for the $W^\pm$ self-energy $(1-\Delta r_W)$ (Ref. 6). The numerical value of Δr_W is

$$\Delta r_W = 0.0713 \pm 0.0013 ,$$

and the masses of the top quark and the Higgs scalar are taken, respectively, as 45 and 100 GeV (Ref. 7). A correction of similar physical origin appears in the electroweak radiative corrections of the asymmetry $A_{\mu\mu}$. The Z^0 propagator is modified by the self-energy of the Z^0. We denote this correction by Δr_Z. Since this correction has the same dependence on the unknown top-quark and Higgs-scalar masses, it is advantageous not to correct the measurements of the asymmetry for the self-energy of the Z^0, but to compare the data to a modified prediction of the standard model, which is

$$A'_{\mu\mu} = \frac{A_{\mu\mu}}{1-\Delta r_Z} . \tag{11}$$

With Eqs. (5) and (10) we rewrite the prediction of the asymmetry given in Eq. (7) in terms of the Fermi constant G_F and obtain[8]

$$A'_{\mu\mu} = -\frac{3G_F g_A^e g_A^\mu}{4\sqrt{2}\pi\alpha} \frac{m_{Z^0}^2 s}{m_{Z^0}^2 - s} \frac{1-\Delta r_W}{1-\Delta r_Z} . \tag{12}$$

This prediction must be compared to measurements of the asymmetry which are not corrected for the self-energy of the Z^0. The radiative corrections Δr_W and Δr_Z are practically identical, and hence cancel out in Eq. (12). Therefore the predicted asymmetry is independent of the self-energies of the weak-gauge bosons. At PETRA energies the asymmetry is insensitive to the precise value of the Z^0 mass. Consequently Eq. (12) must agree with the measurements if the standard model is correct. Experimental values which differ from the predictions of Eq. (12) cannot be explained by a change of the values of the electroweak parameters m_{Z^0} or $\sin^2\theta_W$ or by a modification of the radiative correction arising from a heavy lepton or top quark of high mass. In conclusion, this is one of the most stringent tests of the standard model in the neutral-current sector. (See Behrends and Böhm in Ref. 4.)

A description of the Mark J detector, including the details of triggering, selection, background suppression, cuts, and acceptance can be found in previous publications.[9] We note here that the background contribution from the reactions

$$e^+e^- \to e^+e^-\mu^+\mu^-$$

and

$$e^+e^- \to \tau^+\tau^- \tag{13}$$

are about the 1% level since the cuts

$$\max(p_{\mu^+}, p_{\mu^-}) > \tfrac{1}{2}E_{\text{beam}}$$

and

$$\text{acollinearity } \xi,\ 0 \le \xi \le 20^\circ \tag{14}$$

are efficient in removing these background events, as verified by Monte Carlo studies. We note that the detector acceptance is large $\geq 90\%$ over the interval $-0.8 \le \cos\theta \le +0.8$. θ is the angle between the e^- beam and the μ^-. The probability for charge confusion of the muons (that is, the fraction of like-charge events) is $\sim 1\%$; hence, double-charge confusion is negligible.

For the total-cross-section determination, which is to be compared to Eq. (3), the measured data are corrected for acceptance and the full one-loop electroweak radiative effects. The systematic error arises from two sources: approximately 1% from details of the backgrounds and detector-acceptance uncertainties, and $\sim 3\%$ from the normalization uncertainty in the luminosity. Between neighboring energy points, the luminosity uncertainty is much smaller. This can be seen, for example, by comparing in Table I the data from the two energies 34.6 and 35 GeV, which were taken four years apart. Table I displays all of the Mark J data on $R_{\mu\mu}$. New unpublished data are at 35 GeV, and above 42 GeV there are factor-2 additional events. The data are plotted in Fig. 2 including statistical errors. (Reference 7 has an exhaustive list of references of measurements of $R_{\mu\mu}$ and $A_{\mu\mu}$.)

The measured differential cross-section data are given in Fig. 3 for the combined energies 34.6 and 35 GeV. The data points have been corrected for detector-acceptance and electroweak radiative effects. The dashed line is the symmetric QED cross section and the solid line is fitted to the data by the asymmetric form

TABLE I. $R_{\mu\mu}$ values. The integrated luminosity, number of events, and measured $R_{\mu\mu}$ values at different c.m. energies $\sqrt{s}$.

$\sqrt{s}$ (GeV)	$\int L\,dt$ (pb^{-1})	$N_{\mu\mu}$	$R_{\mu\mu}$
14.0	1.5	472	1.04±0.05
22.5	3.0	357	1.02±0.05
34.6[a]	76.3	3658	0.98±0.016
35.0[b]	68.0	3196	1.00±0.018
36.4	1.4	65	1.08±0.13
38.3	9.5	403	1.07±0.05
40.4	2.6	87	0.93±0.10
42.0	3.4	116	1.04±0.09
43.8	37.5	1123	0.99±0.03
46.1	5.9	155	0.96±0.08

[a]Run 1.
[b]Run 2.

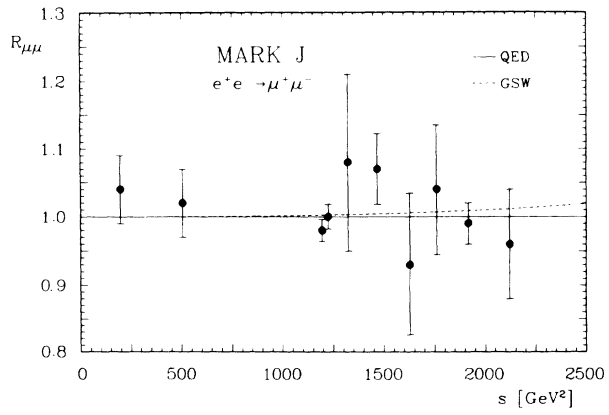

FIG. 2. Measured $R_{\mu\mu}$ values. Statistical errors are shown.

$$\frac{d\sigma_{\mu\mu}}{d\Omega} \propto (1+\cos^2\theta+B\cos\theta) \ . \tag{15}$$

This is the lowest-order form for the cross section.

Table II contains the measured values of the asymmetry $A_{\mu\mu}$ corrected for electroweak radiative effects, detector acceptance, and extrapolated to the full range of $\cos\theta$ ($|\cos\theta|<1$). The quoted error is statistical. The systematic error ($\pm 0.5\%$) is from detector-asymmetry measurement.

The data are plotted in Fig. 4 and compared to the standard model, Eq. (7), with $\sin^2\theta=0.23$ and $m_{Z^0}=91.9$ GeV. It is clear that the measured values at the different energies agree very well with the expected behavior from the standard model. QED alone cannot account for the data. The interference between QED and the weak interaction in the standard model is impressively confirmed by the data. In fact, this is a strong test of the standard model of Glashow, Weinberg, and Salam.

We note from Eqs. (3), (6), and (7) that $A_{\mu\mu}$ and $R_{\mu\mu}$

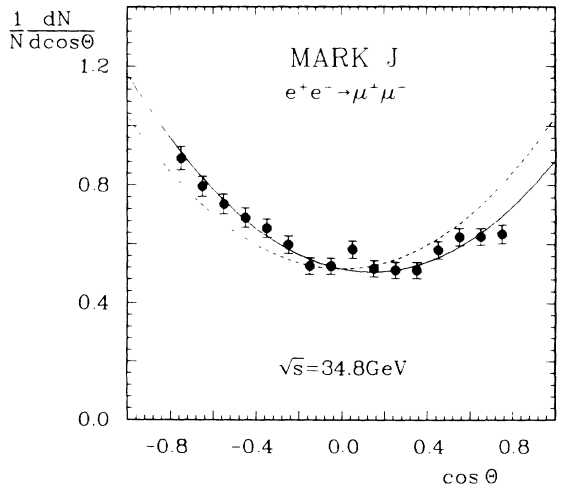

FIG. 3. The differential cross section for $e^+e^- \to \mu^+\mu^-$ at $\sqrt{s}=34.8$ GeV.

TABLE II. $A_{\mu\mu}$ values. Measured $A_{\mu\mu}$ values compared with the standard-model prediction at different c.m. energies $\sqrt{s}$.

$\sqrt{s}$ (GeV)	$\int L\,dt$ (pb^{-1})	$A_{\mu\mu}$ (%)[a]	$A_{\rm GSW}$ (%)
14.0	1.5	+5.3±5.0	−1.2
22.5	3.0	−4.3±6.1	−3.3
34.8	144.3	−10.4±1.3	−8.6
36.4	1.4	−13.6±13.5	−9.5
38.3	9.5	−12.3±5.3	−10.7
40.4	2.6	+5.0±10.5	−12.2
42.0	3.4	−15.9±9.3	−13.4
43.8	37.5	−15.6±3.0	−14.9
46.1	5.9	−17.6±8.3	−17.0

[a]±0.5% systematic error.

depend upon the electroweak parameters $\sin^2\theta_W$ and m_{Z^0}. We cannot obtain independent values of these parameters, essentially because $R_{\mu\mu}$ has errors larger than the predicted difference between its QED value of unity and the electroweak values. However we can construct contours in the $\sin^2\theta_W$-m_{Z^0} plane using a χ^2 function with $\sin^2\theta_W$ and m_{Z^0} as variables. Figure 5 displays the 68%- and 95%-confidence-level (-C.L.) contours for the Mark J data, as well as two data points from the CERN experiments of the UA1 and UA2 Collaborations.[10] The $\sin^2\theta_W$ values for these two experiments were derived using Eq. (5). The error bars drawn in Fig. 5 for the UA1 and UA2 measurements have been increased by a factor of 1.5 in order to correspond to the 68%-confidence-level contour for a simultaneous measurement of two parameters and to correspond to the 68%-C.L. contours given for the Mark J measurement. The agreement is excellent between these experimental determinations. If one of the parameters is fixed at the world value,[7] the other can be evaluated:

$$\sin^2\theta_W=0.21^{+0.04}_{-0.02}\pm 0.01 \quad \text{for } m_{Z^0}=91.9\pm 2 \text{ GeV} \ ,$$

or (16)

$$m_{Z^0}=89^{+4}_{-3}\pm 1 \text{ GeV} \quad \text{for } \sin^2\theta_W=0.230\pm 0.005 \ .$$

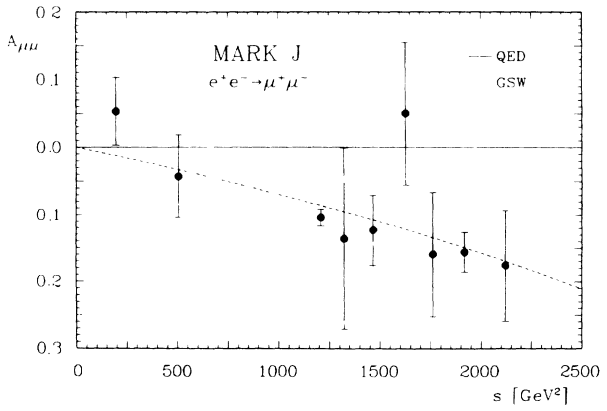

FIG. 4. Measured $A_{\mu\mu}$ values. Statistical errors are shown.

TABLE III. $\sin^2\theta_W$ values. Measured values of $\sin^2\theta_W$ by different experiments and techniques.

Experiment	Method	$\sin^2\theta_W$
Mark J	$e^+e^-\to\mu^+\mu^-$	$0.21^{+0.04}_{-0.02}\pm0.01$
PETRA and PEP	$e^+e^-\to\mu^+\mu^-$	$0.20\pm0.02\pm0.01$
UA1	$1-(m_W/m_Z)^2$	0.194 ± 0.032
	$(38.65\ \text{GeV}/m_W)^2$	$0.214\pm0.006\pm0.015$
UA2	$1-(m_W/m_Z)^2$	$0.232\pm0.025\pm0.010$
	$(38.65\ \text{GeV}/m_W)^2$	$0.232\pm0.003\pm0.008$
CCFRR	$\sigma^{NC}_{\nu N}/\sigma^{CC}_{\nu N}$	$0.242\pm0.011\pm0.005$
CDHS	$\sigma^{NC}_{\nu N}/\sigma^{CC}_{\nu N}$	$0.225\pm0.005\pm0.006$[a]
CHARM	$\sigma^{NC}_{\nu N}/\sigma^{CC}_{\nu N}$	$0.236\pm0.005\pm0.006$[a]
FMM	$\sigma^{NC}_{\nu N}/\sigma^{CC}_{\nu N}$	$0.247\pm0.012\pm0.013$
CHARM and $E734$	$\sigma_{\nu_\mu e^-}/\sigma_{\bar\nu_\mu e^-}$	$0.212\pm0.021\pm0.009$

[a]Theoretical error includes c-quark mass $m_c=(1.5\pm0.4)$ GeV.

The second error is an upper bound for the systematic error. The determination of $\sin^2\theta_W$ involves only neutral-current interactions of leptons and the measurements of the W and Z masses. It avoids the complications arising in the measurements of $\sin^2\theta_W$ using nuclear targets. This measurement of $\sin^2\theta_W$ is at high energy and is thus complimentary to the low-energy neutrino-electron elastic-scattering determination of $\sin^2\theta_W$ which is also purely leptonic in nature.[11] Note in Fig. 5 the dashed curve is a plot of the equation

$$m^2_{Z^0}=\frac{\pi\alpha}{\sqrt{2}G_F\sin^2\theta_W\cos^2\theta_W}\frac{1}{1-\Delta r_W} \tag{17}$$

which is derived from Eqs. (5) and (10).

Tables III and IV compare the Mark J results for $\sin^2\theta_W$ and m_{Z^0} with the world values from combining data from similar experiments and also with different experiments.[12]

The rows labeled PETRA and PEP include data from the CELLO, JADE, Mark J, PLUTO, and TASSO Collaborations at PETRA, the Mark I Collaboration at the SLAC storage ring SPEAR, and the HRS, MAC, and Mark II Collaborations at the SLAC storage ring PEP. The consistency of the results is remarkable.

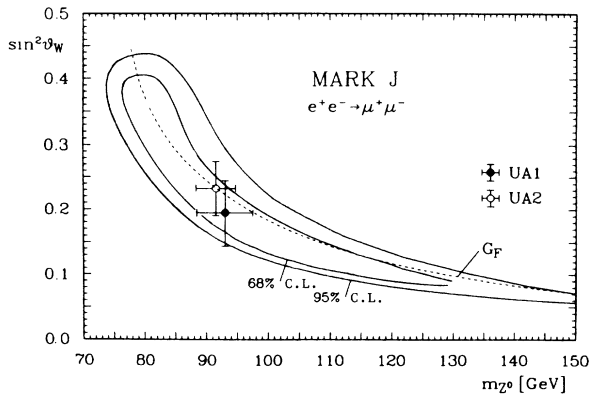

FIG. 5. Calculated contours in the $\sin^2\theta_W$-m_{Z^0} plane.

It is also possible, using the total cross section and the asymmetry at each energy, to determine the vector and axial-vector coupling constants of the muon. The measurement of $R_{\mu\mu}$ determines mainly the product $g^e_V g^\mu_V$ and measurement of $A_{\mu\mu}$ the product $g^e_A g^\mu_A$, as can be seen from Eqs. (3) and (7). We rewrite the parameter χ defined in Eq. (6) in terms of G_F using Eqs. (5) and (9) and obtain

$$\chi=\frac{G_F}{2\pi\alpha\sqrt{2}}\frac{m^2_{Z^0}s}{m^2_{Z^0}-s}\frac{1-\Delta r_W}{1-\Delta r_Z}\ . \tag{18}$$

In this parametrization we have included the radiative corrections Δr_W and Δr_Z in the same way as in the asymmetry given by Eq. (12) in order to cancel the corrections due to the self-energy of the bosons. The use of this parametrization of χ in the prediction of $R_{\mu\mu}$ and of $A_{\mu\mu}$ has the advantage that the resulting predictions are very insensitive to parameters other than the vector and axial-vector couplings of the electron and the muon. In the asymmetry we obtain Eq. (12), in which we have not written the purely weak terms for simplicity, but they are included in the determination of the electroweak parameters. Note that we must not correct the measurements of $R_{\mu\mu}$ and $A_{\mu\mu}$ for the self-energy of the Z^0 when we compare measurement to the prediction using Eq. (18), since it is already included in the theoretical prediction.

From the Mark J data we obtain

$$g^e_V g^\mu_V=0.04^{+0.04}_{-0.02}$$

and (19)

$$g^e_A g^\mu_A=0.280\pm0.015\ ,$$

TABLE IV. m_{Z^0} values. A comparison of measured m_{Z^0} values from different experiments.

Experiment	Method	m_{Z^0} (GeV)
Mark J	$e^+e^-\to\mu^+\mu^-$	$89^{+4}_{-3}\pm1$
PETRA and PEP	$e^+e^-\to\mu^+\mu^-$	$88\pm2\pm1$
UA1	$p\bar p\to Z^0+X$	$93.0\pm1.4\pm3.0$
UA2	$p\bar p\to Z^0+X$	$91.5\pm1.2\pm1.7$

and the errors are those from independent measurements of each parameter. In the standard model [Eq. (4)] we expect

$$g_V^e g_V^\mu = 0.002 \quad (\sin^2\theta_W = 0.23)$$

and (20)

$$g_A^e g_A^\mu = 0.25 \ .$$

The agreement is very good between our values and the standard-model expectations. Combining all $\mu\mu$ data from PETRA and PEP the values of the coupling constants are[13]

$$g_V^e g_V^\mu = 0.04^{+0.05}_{-0.03}$$

and (21)

$$g_A^e g_A^\mu = 0.283 \pm 0.023 \ .$$

In the standard model only one Higgs doublet is involved. For models with a Higgs structure more complicated than doublets or in theories having additional neutral-vector bosons, Eq. (12) is modified by a parameter ρ which multiplies the right side of that equation, and Eq. (5) becomes

$$\rho = \frac{m_{W^\pm}^2}{m_{Z^0}^2 \cos^2\theta_W} \ . \tag{22}$$

From our data and the modified Eq. (12), including ρ, we find

$$\rho = 1.08 \pm 0.10 \pm 0.03 \ , \tag{23}$$

which is nearly independent of $\sin^2\theta_w$ and m_{Z^0}. This determination is free of the uncertainty in the top-quark mass. It is a powerful test of the simple standard model.

III. $e^+e^- \to \tau^+\tau^-$

We have studied τ-lepton production over the c.m. system (c.m.s.) energy region from 14 to 46.8 GeV (Ref. 14). The data reported here have an integrated luminosity of 214 pb^{-1}. τ leptons are detected by their decay products, since their decay path is very short. In the Mark J detector, the cleanest reaction is the channel $e^+e^- \to \tau^+\tau^- \to \mu^\pm \nu\bar{\nu} + X^\mp$, where $X = e\nu\bar{\nu}$ or hadrons + ν. Results are given on (1) the cross section, (2) the decay branching ratio into $\mu\nu\bar{\nu}$, and (3) the electroweak parameters.

The selection of events and the understanding of the potential sources of background are crucially important. These are discussed in detail in Refs. 14 and 9. It is clear that the collinearity of the production process and the missing energy due to the emission of neutrinos are the major factors in selecting events. The acollinearity angle between muon and jet must be less than 30°. The selection criteria yield a sample of 2197 $\tau\tau \to \mu X$ events. The overall detection efficiency including geometrical acceptance and kinematical cuts is center-of-mass energy dependent. Note that the acceptance is calculated with all radiative events (to order α^3) included. The kinematic cuts preferentially remove hard-radiative events, thus the overall acceptance appears small, 40% to 40 GeV. The entire background is less than 5% of the final-data sample, and the major contribution is from $e^+e^- \to \mu^+\mu^-\gamma$ events.

The cross section for τ-pair production with the required decay characteristics is experimentally determined by

$$\sigma(\tau\tau \to \mu X) = \frac{N}{\epsilon L} \ , \tag{24}$$

where N is the number of observed τ events minus the number of expected background events and ϵ is the total acceptance. L is the integrated luminosity. The total cross section for τ-pair production is

$$\sigma(\tau\tau) = \frac{\sigma(\tau\tau \to \mu X)}{2B(\tau \to \mu)[1 - B(\tau \to \mu)]} \ . \tag{25}$$

$B(\tau \to \mu)$ is the branching ratio for the τ decay to muon ($\tau \to \mu\nu\bar{\nu}$). The weak correction to the QED prediction is small. However, the first-order QED radiative correction $\delta_{\rm em}^\gamma$ to the one-photon-exchange diagram is large ($\delta_{\rm em}^\gamma \approx 35\%$ for $\sqrt{s} = 35$ GeV) and is included. This correction is before kinematical cuts are applied. After cuts, the actual correction to accepted events is about 10%, since the hard radiative events are, in large measure, eliminated by the cuts. We normalize the measured cross section $\sigma(\tau\tau)$ to the QED cross section calculated to $O(\alpha^3)$ so that variations from the QED prediction will be seen as a deviation from unity. Thus to $O(\alpha^3)$ we have

$$\begin{aligned} R(\tau\tau) &= \frac{\sigma(\tau\tau)}{\sigma_{(\tau\tau)}^{\rm QED}} \\ &= \frac{\sigma(\tau\tau)}{\sigma_0^{\rm QED}(1+\delta_{\rm em}^\gamma)} \\ &= \frac{N}{\sigma_0^{\rm QED}\epsilon(1+\delta_{\rm em}^\gamma)L} \frac{1}{2B(\tau \to \mu)[1 - B(\tau \to \mu)]} \ . \end{aligned} \tag{26}$$

Any variation from the QED prediction shows up as a deviation of $R(\tau\tau)$ from unity. The values of $R(\tau\tau)$ as a function of $\sqrt{s}$ are shown in Table V, where $B(\tau \to \mu)$ was taken as 17.6%. The systematic error on $R(\tau\tau)$ is 5%, mainly from the uncertainty in the luminosity measurement. Clearly the data are consistent with $R(\tau\tau) = 1$. Figure 6 is a plot of data in Table V. The solid line is the QED prediction, and the dashed lines are given using the derived cutoff values Λ for the assumed form factor for the τ. The lower is $\Lambda^- > 206$ GeV, the upper $\Lambda^+ > 262$ GeV. Figure 7 presents the R values from all PETRA and PEP experiments.[15]

If we require $R(\tau\tau)$ to be unity, then from Eq. (25) we find

$$B(\tau \to \mu) = (17.4 \pm 1.0)\% \ . \tag{27}$$

Both statistical and systematic errors are included. This value agrees well with the world average of 17.6±0.4%. Our sample of this τ-decay channel is the largest yet reported.[16]

Only events with $|\cos\theta| < 0.8$ were included in the

TABLE V. $R_{\tau\tau}$ values. The integrated luminosity, number of events, and measured $R_{\tau\tau}$ values at different c.m. energies $\sqrt{s}$.

$\sqrt{s}$ (GeV)	$\int L\,dt$ (pb^{-1})	$N(\tau\to\mu\nu\bar{\nu})$	$R(\tau\tau)$[a]
14.0	1.57	79	1.13±0.14±0.07
22.4	3.87	92	1.02±0.12±0.06
⟨34.7⟩	148.45	1551	1.00±0.03±0.05
⟨39.4⟩	16.49	144	0.98±0.08±0.05
43.8	37.83	287	0.97±0.06±0.05
46.1	5.85	44	1.02±0.16±0.05

[a]The first error is statistical, the second systematic.

data sample for the angular distribution. This criterion ensures a uniform acceptance over the complete angular region. We use data above 30 GeV since it has an equal amount of luminosity at both magnet polarities and systematic effects due to detector asymmetries cancel out. The original τ direction was estimated by the vectorial difference of the muon momentum and the energy of the jet. The original flight direction of the τ is known from this procedure to a precision of 2.5°. The measured differential cross section at 34.7 GeV is shown in Fig. 8. The data are corrected for acceptance and $O(\alpha^3)$ QED radiative effects as explained in Sec. II. Following the method outlined there for muon pairs, we determine the forward-backward asymmetry of τ's over the full angular range:

$$34.7\ \text{GeV, 1401 events,}\quad A_{\tau\tau}=-10.6\pm3.1\%(-8.5\%)\ , \tag{28}$$

$$43.8\ \text{GeV, 287 events,}\quad A_{\tau\tau}=-8.5\pm6.6\%(-15.4\%)\ .$$

The values in parentheses are the standard-model predictions using $\sin^2\theta_w=0.23\pm0.005$ and $m_{Z^0}=91.9\pm2$ GeV. The errors shown are statistical. Systematic errors are at the 1.5% level, resulting from detector asymmetry (±0.05%), charge confusion (<1%) and QED-induced asymmetry (<0.2%). Figure 9 plots $A_{\tau\tau}$ values from PETRA and PEP experiments.

Our measurements of $A_{\tau\tau}$ and $R_{\tau\tau}$ can be used to determine the vector and axial-vector neutral-current coupling-constant products. We find the values

$$g_V^e g_V^\tau=0.07\pm0.07\ \ (0.02\pm0.03)\ ,$$

$$g_A^e g_A^\tau=0.223\pm0.064\ \ (0.227\pm0.016)\ .$$

The errors include both statistical and systematic errors on $A_{\tau\tau}$ and $R_{\tau\tau}$ and the above-quoted errors on $\sin^2\theta_W$ and m_{Z^0}. The values in parentheses are the PETRA and PEP averaged values.

The τ data, that from the Mark J alone, or the combined PETRA and PEP data, strongly support lepton universality and the standard-model predictions.

IV. $\mu^+\mu^-\gamma$

A study of $\mu^+\mu^-\gamma$ events provides a method of testing the validity of electroweak theory at higher order. As in the $\mu^+\mu^-$ channel, the Z^0 exchange does not significantly effect the total cross section, but it does effect the forward-backward muon asymmetry. The photon can simply be classified as being radiated either in the initial or the final state. Interference between the initial- and the final-state radiation does not contribute to the QED total cross section because it is antisymmetric. We also

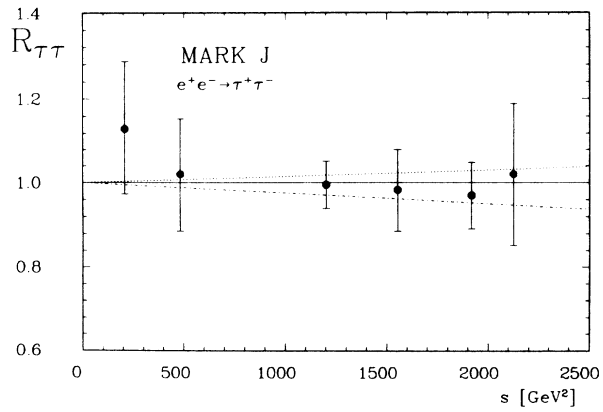

FIG. 6. Measured $R_{\tau\tau}$ values. Statistical errors are shown.

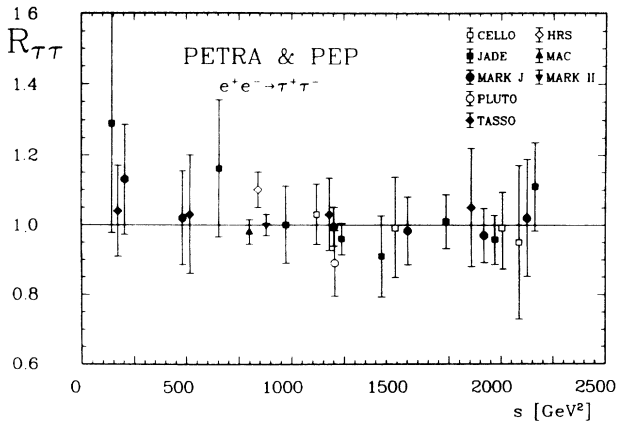

FIG. 7. $R_{\tau\tau}$ data from all PETRA and PEP experiments.

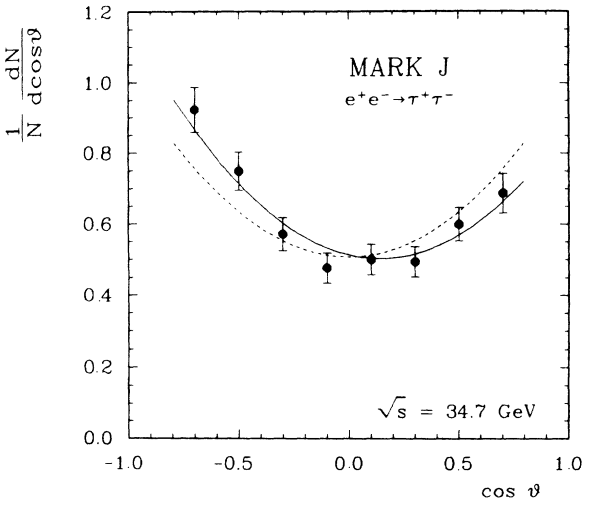

FIG. 8. The measured angular distribution for $e^+e^- \to \tau^+\tau^-$ corrected for QED contributions to $O(\alpha^3)$ for $\sqrt{s} = 34.7$ GeV. The solid line is the best fit to the data including electroweak interference. The dashed line is the lowest-order QED prediction.

note that the photons radiated in the initial (final) state tend to go in the direction of the electron beams (muons); hence, the angular distribution is quite sensitive to the cuts applied to obtain the distribution. Figure 10 is the angular distribution of the photon obtained by applying the following cuts to the Monte Carlo events:

$$\begin{aligned} &\mathrm{Max}(p_+, p_-) \geq E_b/3 \ , \\ &\xi(\text{acollinearity}) \leq 160^\circ \ , \\ &|\cos\theta_\mu| \leq 0.8 \ , \\ &E_\gamma \geq 0.03\sqrt{s} \ . \end{aligned} \tag{29}$$

From Fig. 10, it is clear that when we impose the condition that $|\cos\theta_\mu| \leq 0.8$ in our accepted event sample, the final-state radiation is a factor of 2 larger than the initial-state radiation. We also note that events with very energetic photons are always accompanied by a pair of muons which are at small angles with one another. Some of these events are lost since the detectors cannot always resolve the muons. The $\mu^+\mu^-\gamma$ events are selected using these criteria in addition to those in Eq. (29)

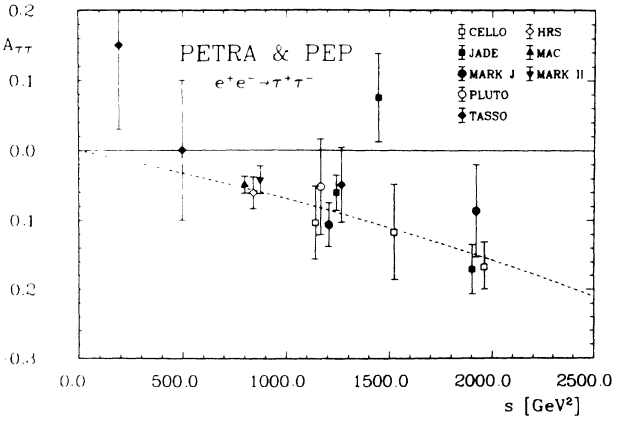

FIG. 9. The charge asymmetry $A_{\tau\tau}$ as a function of s from PETRA and PEP experiments. The solid line is the QED prediction and the dashed line the standard-model prediction with $\sin^2\theta_w = 0.23$ and $m_{Z^0} = 91.9$ GeV.

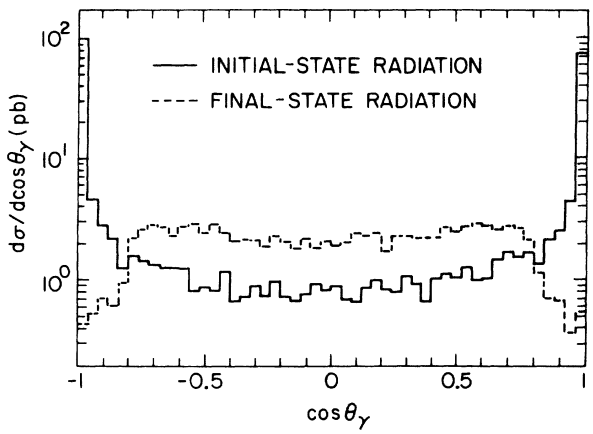

FIG. 10. For $e^+e^- \to \mu^+\mu^-\gamma$, the photon angular distribution of the initial- and final-state radiation. Cuts are given in the text.

(1) There are two coincident muon-trigger counter hits and two drift-chamber tracks coming from the interaction point.

(2) The direction of the electromagnetic shower is computed with the assumption that the particle is from the vertex point. The energy of a shower which is collinear with one of the muons ($\theta_{\mu\gamma} \leq 5^\circ$) is required to be larger than $6\%\sqrt{s}$. This reduces the effect of the minimum-ionizing energy left by the muon.

(3) There must not be a drift-tube track associated with the electromagnetic shower, if the shower is not collinear ($\theta_{\mu\gamma} \leq 10^\circ$) with the muon track.

(4) The acceptance of the shower is limited to $|\cos\theta_\gamma| \leq 0.9$.

(5) The drift tubes do not cover $\pm 7^\circ$ at the four corners ($\phi = \pm 45^\circ$) above and below the particle-orbit plane; hence, events in electromagnetic showers at these positions are not included.

(6) Coplanarity is assured by requiring the opening angles to satisfy $360^\circ - (\theta_{\gamma\mu^-} + \theta_{\gamma\mu^+} + \theta_{\mu\mu}) \leq 5^\circ$.

Taking advantage of the good muon angular resolution of the Mark J detector, the momenta or energy of the muons and photon can be most precisely reconstructed from the orientation of the muons and photon using energy and momentum conservation. The greatest uncertainty is in the measurement of the direction of the photon. If the photon is collinear with a muon, E_γ is determined from the calorimeter energy. The uncertainty in the invariant $\mu\gamma$ mass is estimated to be about 3% at 35 GeV from a Monte Carlo study.

The backgrounds are from the following sources.

(1) The two-photon reaction $e^+e^- \to e^+e^-\mu^+\mu^-$, in

TABLE VI. A comparison of the number of observed and calculated (Monte Carlo) $\mu^+\mu^-\gamma$ events.

Energy band (GeV)	$(\sqrt{s})$ (GeV)	$\int L\,dt$ (pb^{-1})	N (obs)	N (MC)
28.7–37.0	34.7	120	568	580
37.0–46.0	42.8	60	227	231

which only one electron is detected in the electromagnetic calorimeter, but its track is not reconstructed in the drift tubes.

(2) τ-pair production, in which one τ decays into a muon and the other into hadrons, one of which punches through the hadron calorimeter and triggers a muon counter.

(3) $\tau\tau\gamma$ events, in which the τ's decay into muons.

(4) $e^+e^-\mu^+\mu^-\gamma$ events in which both electrons are not detected.

Monte Carlo studies simulate these processes and estimate their acceptance. Monte Carlo events are passed through the analysis programs and are visually scanned as are the real-data events. The contamination from the processes above is less than 1%.

This experiment has accumulated a much larger set of events in the $\mu^+\mu^-\gamma$ reaction than other published results.[17,18] Table VI shows the observed number of events compared to that expected from our Monte Carlo prediction at mean energies of 34.7 and 42.8 GeV. We find the data in excellent agreement with the electroweak theory to order α^3. We show this agreement in Figs. 11–17.

The photon energy distribution is shown in Fig. 11. It peaks at low energy as expected, but the expected large peak at $E_\gamma = E_{\text{beam}}$ is suppressed by the detector, which cannot resolve very close muon pairs. The acceptance is essentially zero for events in which the muon acollinearity is larger than 160°. This distribution is given in Fig. 12. Figure 13 is a plot of the muon-pair invariant mass normalized to the center-of-mass energy $\sqrt{s}$. Figure 14 is the $\mu\gamma$ invariant-mass plot. Since the radiated photon

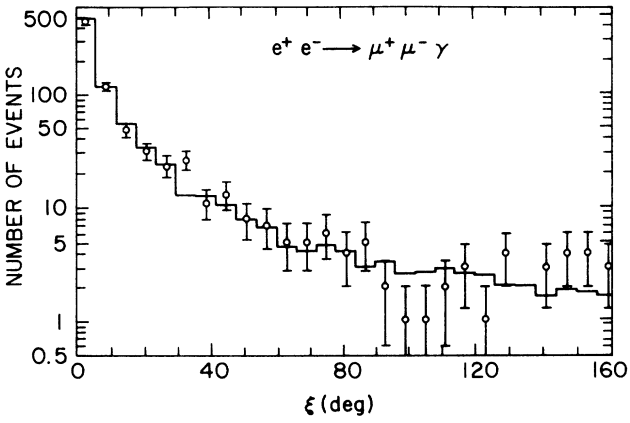

FIG. 12. The muon acollinearity distribution in $\mu^+\mu^-\gamma$.

tends to be in the low-energy region and collinear with one of the muons, the normalized $\mu\gamma$ invariant-mass distribution shows peaks at 0 and 0.25. Figure 15 is the $\mu\gamma$ opening angle distribution.

The muon charge asymmetry in the $\mu^+\mu^-\gamma$ reaction arises from the electroweak interference and also from the QED interference between the photons radiated in the initial and final states. These differ in their dependence upon the kinematic cuts. The asymmetry from the electroweak interference is more or less independent of the cuts since it depends essentially upon the momentum transfer of the virtual Z^0, while it is easily seen that the QED interference is extremely sensitive to the kinematic cuts. For example, the QED interference decreases as the photon energy increases. Figure 16 shows this general dependence. The angular distribution of the produced muons with respect to the beam direction is shown in Fig. 17. Each event has two entries: one from the angle of the μ^- with respect to the e^- beam and one from the angle of the μ^+ with respect to the e^+ beam. The asymmetry is defined as

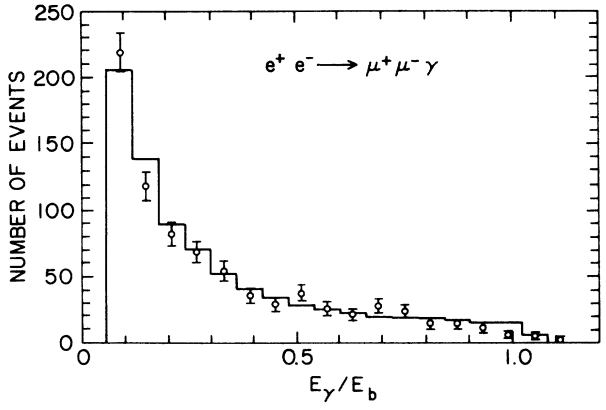

FIG. 11. The photon energy distribution in $\mu^+\mu^-\gamma$.

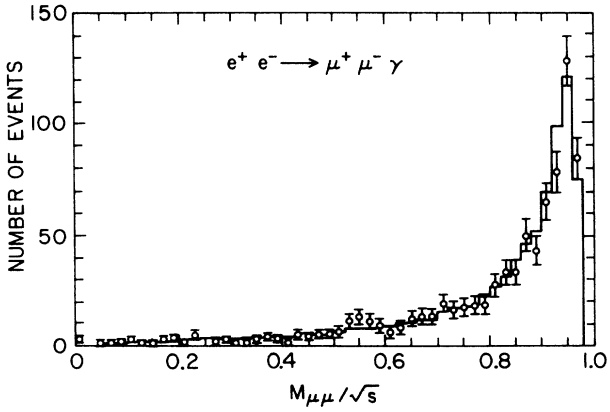

FIG. 13. The muon-pair invariant-mass distribution in $\mu^+\mu^-\gamma$.

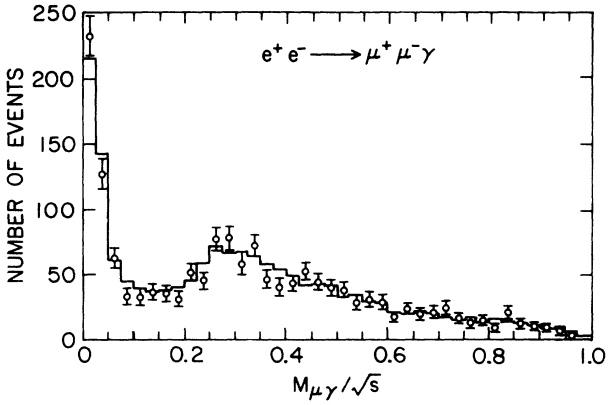

FIG. 14. The $\mu\gamma$ invariant-mass distribution in $\mu^+\mu^-\gamma$.

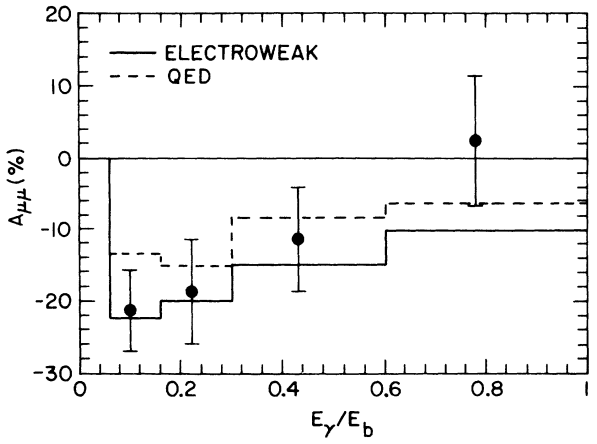

FIG. 16. The muon charge asymmetry as a function of photon energy in $\mu^+\mu^-\gamma$.

$$A=\frac{N(\theta<90^\circ)-N(\theta>90^\circ)}{N(\theta<90^\circ)+N(\theta>90^\circ)}\ , \tag{30}$$

where N is the number of muons. The observed and expected asymmetries (%) are

$$A(\text{observed})=-14.7\pm3.5(\text{statistical})\pm1.0(\text{systematic})\ ,$$

$$A(\text{electroweak})=-18.4\pm1.3\ ,$$

$$A(\text{QED})=-11.6\pm1.3\ .$$

The systematic error in A(observed) is from detector asymmetry We note that two-thirds of the predicted asymmetry is from the QED part alone. The QED asymmetry of the $\mu\mu\gamma$ events together with virtual-photon processes, to order α^3, has been used as a correction to the electroweak asymmetry of the dimuon sample. The correction is small (about 1% under kinematic cuts) as a result of the cancellation between the asymmetry of the $\mu\mu\gamma$ events and that of virtual-photon processes. Hence, it is essential to be able to separate the contributions and test the calculations. Our measurement of the asymmetry of $\mu\mu\gamma$ events confirms the validity of the QED calculation. The agreement with the electroweak theory is good for all of the distributions which we have shown, including the asymmetry as well.

In all Monte Carlo simulations, only the lowest-order diagrams for radiative muon-pair production are included. Depending upon the kinematic cuts, the higher-order corrections are estimated to be about ±3% for the cross section and less than 1.5% for the charge asymmetry in the acceptance.

V. $e^+e^-\mu^+\mu^-$

This two-photon production process can be used to test QED to order α^4. In particular, the experimental groups at PETRA have data up to 46.8 GeV and thus data at larger values of Q^2 (the square of the four-momentum

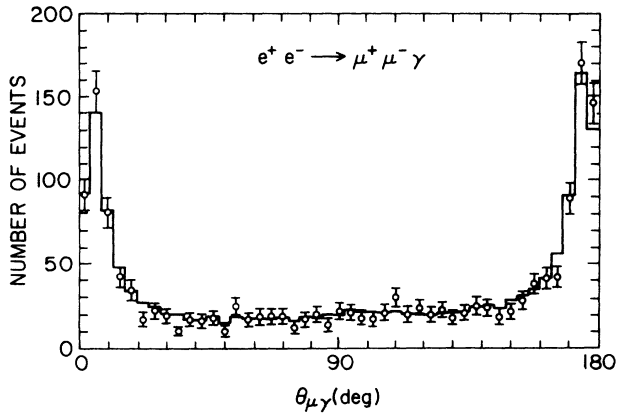

FIG. 15. The $\mu\gamma$ opening-angle distribution in $\mu^+\mu^-\gamma$.

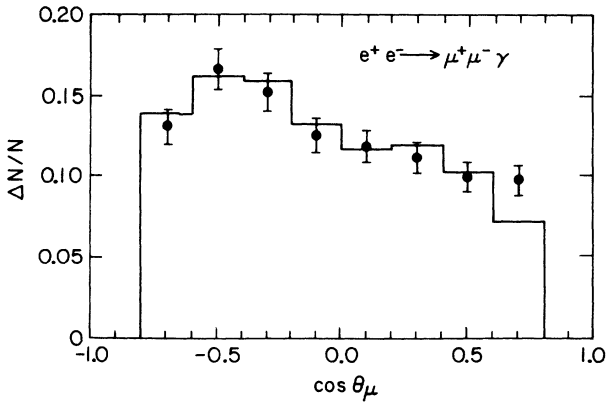

FIG. 17. The muon angular distribution in $\mu^+\mu^-\gamma$. $\Delta N/N$ is the fraction of the sample N in the given $\Delta(\cos\theta_\mu)$ bin.

TABLE VII. Selection criteria for $e^+e^- \rightarrow e^+e^-\mu^+\mu^-$ events.

Category	$P_t(\mu) > 1.5$ GeV	$P(\mu) < 0.5E_b$	E_{em}	Other
$\mu\mu$	≥ 1 muon	2 muons	$< 0.2E_b$	
$e\mu\mu$	≥ 1 muon	≥ 1 muon	$> 0.2E_b$	Unbalanced momentum $> 0.25E_b$
$ee\mu$, $ee\mu\mu$	≥ 1 muon		$> 0.2E_b$	2 tracks in em calorimeter, one electron identified.

transfer between the incoming and outgoing electron), $M_{\mu\mu}$, and P_t (the muon transverse momentum) can be investigated.

The elements of the Mark J detector which were used for this reaction were the drift-tube vertex detector, the electromagnetic calorimeter, the time-of-flight counters, and the muon spectrometer. Details can be found in Ref. 19.

The $ee\mu\mu$ events detected were classified into three categories: (1) $\mu\mu$ (untagged); (2) $e\mu\mu$ (single tagged); and (3) $ee\mu\mu$ and $ee\mu$ (double tagged). To distinguish two-photon muon events from single-photon muon events, we have used the fact that the momentum spectrum of muons from the single-photon process peak at the beam energy while the muons produced in the two-photon interactions have much lower momentum. Figure 18 displays this clearly, and the momentum cut indicated on the figure shows that the contamination from the single-photon $\mu\mu$ interaction is small. The selection criteria are listed in Table VII.

We have studied the contamination from the processes $\mu\mu\gamma$, $\tau\tau\gamma$, and $ee\tau\tau$ QED Monte Carlo events. The result is a background of 1–2.5 % depending upon the type of final state and the center-of-mass energy. These have been subtracted from the data sample.

A complete α^4-order QED Monte Carlo program[20] was used to generate $ee\mu\mu$ events including detector simulation. All interference terms between the Feynman diagrams (Fig. 19) and lepton masses have been included in the calculation. The higher-order radiative correction, estimated to be at the 1% level, is not included.

The observed cross section for $ee \rightarrow ee\mu\mu$ is shown in Fig. 20 as a function of $\sqrt{s}$ for tagged and untagged events separately. The statistical error is given on the data points, and the systematic error is about 4% including errors of luminosity and detector efficiency. $\sigma(\mu\mu)$ increase logarithmically as the energy increases. The measured cross section agrees well with the QED predictions. The number of events in the data and the expected number from a Monte Carlo calculation are shown in Table VIII for $\sqrt{s} > 30$ GeV. The integrated luminosity is 108 pb^{-1}.

Other parametrical distributions agree very well with QED predictions.[21] Figure 21 has the acoplanarity and acollinearity plots for the untagged events at an average $\sqrt{s} = 44$ GeV. Acoplanarity ϕ and acollinearity ξ are defined, respectively, as $\phi = 180°$ minus the angle between the two-muon-momentum projections in the plane perpendicular to the beam axis, and $\xi = 180°$ minus the angle

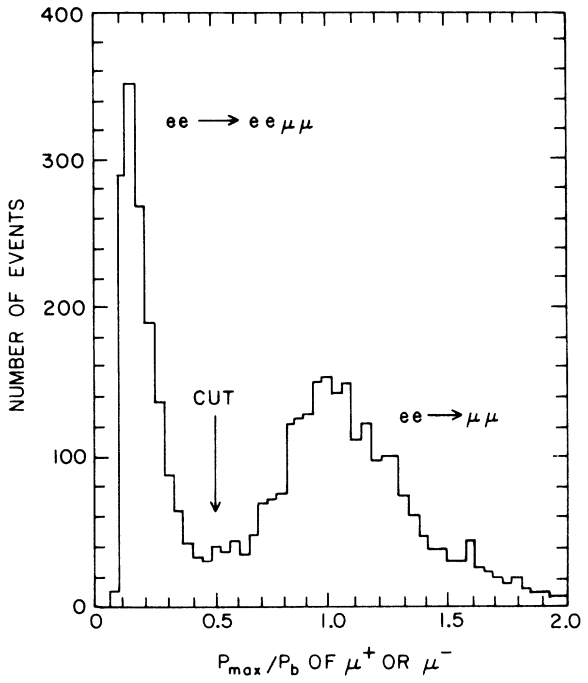

FIG. 18. The maximum momentum P_{max} distribution demonstrates how a cut in P_{max} separates the two-photon channel $e^+e^-\mu^+\mu^-$ from the single-photon channel $\mu^+\mu^-$.

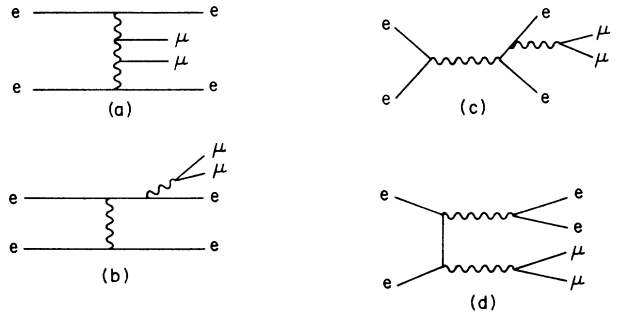

FIG. 19. Feynmam diagrams contributing to $e^+e^- \rightarrow e^+e^-\mu^+\mu^-$: (a) multiperipheral, (b) bremsstrahlung, (c) conversion, and (d) annihilation.

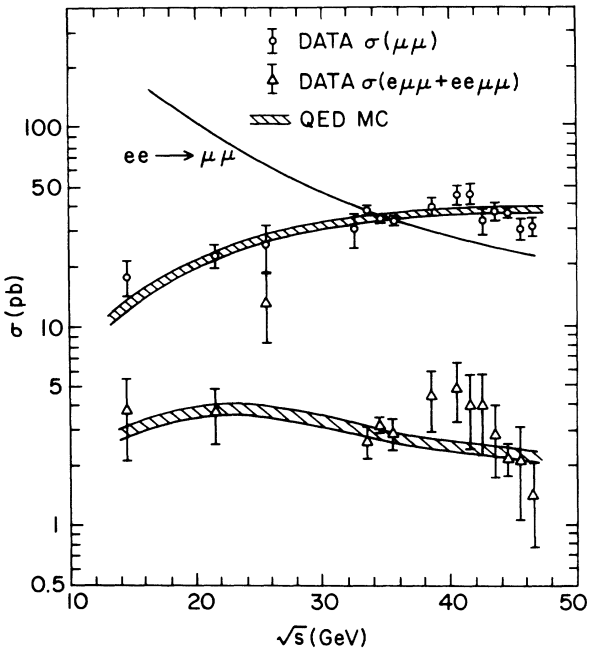

FIG. 20. The measured cross section including acceptance, in pb, for $e^+e^-\to e^+e^-\mu^+\mu^-$ as a function of $\sqrt{s}$. The $e^+e^-\to\mu^+\mu^-$ cross section is given for comparison.

between the directions of the muon momenta. Figure 22 is for the tagged data, including lower energies in order to have the largest number of events possible. We note that QED Monte Carlo calculations fit the data well. The invariant-mass distribution of the two muons is given in Fig. 23 for the single-tagged sample. Again the agreement is good. Similarly, although we do not show them, the untagged invariant-mass distribution and the Q^2 distributions for the tagged events are described well by QED.

The agreement between data and the QED Monte Carlo calculations after detector-response simulation allows us to apply a bin-by-bin acceptance correction to the data. This has been done for the data in Fig. 24 which displays the differential cross section as a function of the muon transverse momentum P_t with respect to the beam line.[22] The data are fit well by a power law

$$d\sigma/dP_t^2 = aP_t^{-b} \tag{31}$$

TABLE VIII. A comparison of the number of $e^+e^-\mu^+\mu^-$ events in the data and the number expected from the Monte Carlo study for $\sqrt{s} > 30$ GeV.

	$\mu\mu$	$e\mu\mu$	$ee\mu$ and $ee\mu\mu$
Data	3671±61	283±17	43±7
MC	3834±31	256±8	39±3

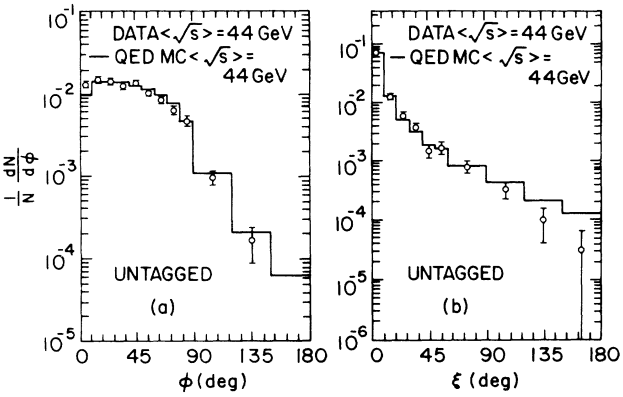

FIG. 21. (a) The acollinearity and (b) acoplanarity for two muons in the untagged case ($40 < \sqrt{s} < 46.78$ GeV).

with $a = 0.45\pm0.07$ nb/(GeV/c)^2 and $b = 4.47\pm0.15$. Also shown in the figure are the predictions of a DEPA (double equivalent-photon approximation)[23] and the QED Monte Carlo prediction, both of which describe the untagged data equally well.

Our study shows that the complete α^4 QED calculation describes the two-photon production data very well over the energy range $14 < \sqrt{s} < 46.8$ GeV and the Q^2 range from 0.7 to 166 GeV^2.

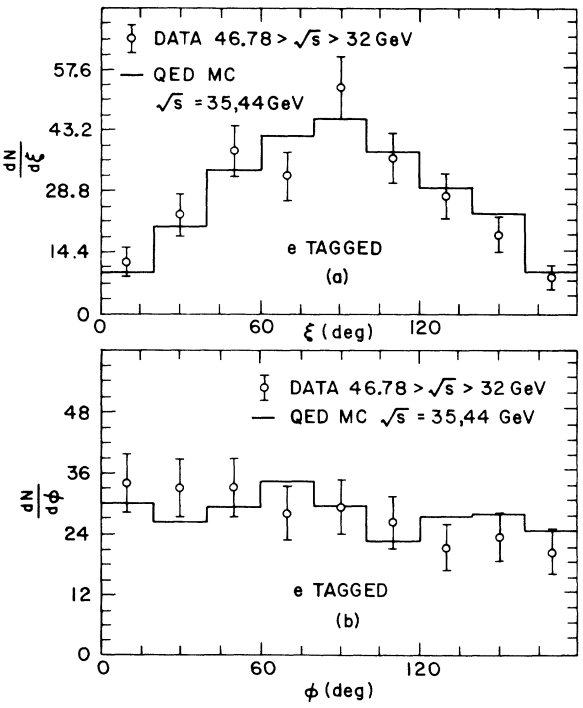

FIG. 22. (a) The acollinearity and (b) acoplanarity for two muons in the single-tagged case ($30 < \sqrt{s} < 46.78$ GeV).

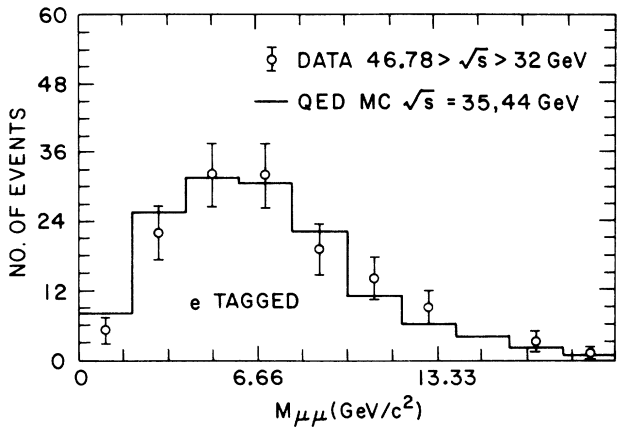

FIG. 23. The invariant-mass distribution of muon pairs in the single-tagged case ($30 < \sqrt{s} < 46.78$ GeV).

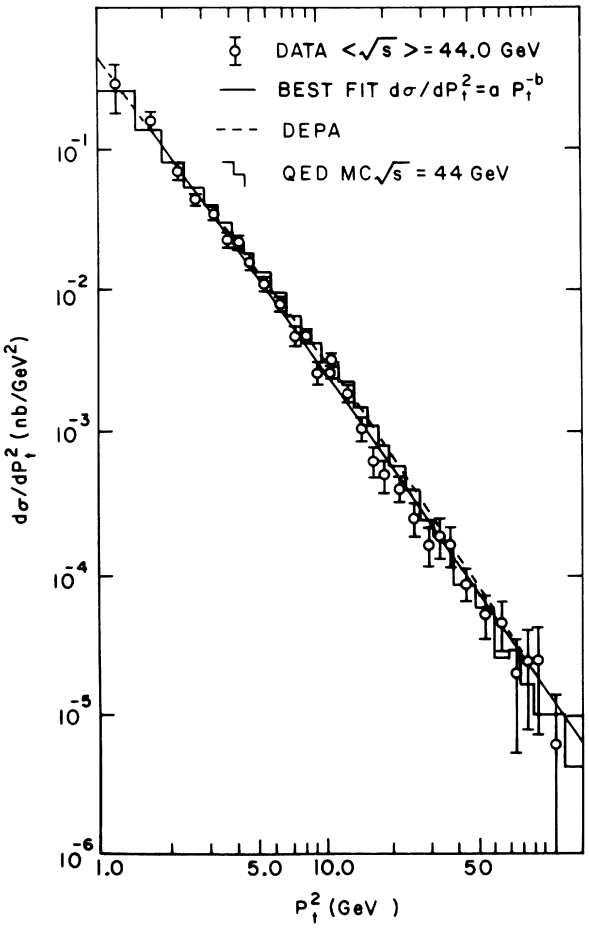

FIG. 24. The differential cross section as a function of the muon transverse momentum squared (two entries per event). The points are data; the solid curve is the best fit to the power law aP_t^{-b}; the dashed curve is the DEPA; the histogram is the α^4 QED Monte Carlo prediction.

VI. SUMMARY

All electroweak data from the Mark J experiment, indeed from all e^+e^- collider experments, agree within experimental uncertainty with the predictions of the standard model. The agreement is striking.

The forward-backward asymmetry data in muon and τ-pair production ($A_{\mu\mu}, A_{\tau\tau}$) as a function of $\sqrt{s}$, is fit precisely by the standard model. From the total cross section $R_{\mu\mu}$ and $A_{\mu\mu}$, we calculate

$$\sin^2\theta_W = 0.21^{+0.04}_{-0.02} \pm 0.01$$

assuming $m_{Z^0} = 91.9 \pm 2$ GeV. Or vice versa, if we use $\sin^2\theta_W = 0.230 \pm 0.005$, the world value using all existing measurements, we determine

$$m_{Z^0} = 89^{+4}_{-3} \pm 1 \text{ GeV} .$$

Parametrizing $A_{\mu\mu}$ as in Eq. (12) and using $R_{\mu\mu}$, we determine the vector and axial-vector couplings in a manner which is insensitive to the mass of the Z^0 and $\sin^2\theta_W$. We obtain

$$g_V^e g_V^\mu = 0.04^{+0.04}_{-0.02} ,$$

$$g_A^e g_A^\mu = 0.280 \pm 0.015$$

in excellent agreement with predictions of the standard model and the combined world data. Comparing this result with that for τ's it is clear that the data strongly support lepton universality.

From the Mark J data, we determine $\rho = 1.08 \pm 0.10 \pm 0.03$, a sharp test of the theory, which is free of the current uncertainty in the top-quark mass.

For the τ-pair production reaction, we find the branching ratio $\tau \to \mu + X = 17.4 \pm 1.0\%$ in excellent accord with the world average of $17.6 \pm 0.4\%$.

In $\mu^+\mu^-\gamma$ production, all measured distributions including the forward-backward asymmetry are in excellent agreement with the electroweak theory.

Our data on the two-photon process $e^+e^- \to e^+e^-\mu^+\mu^-$ agrees in detail with QED to order α^4, over the energy range 14–46.8 GeV and the Q^2 range from 0.7 to 166 GeV^2.

ACKNOWLEDGMENTS

We acknowledge the superb operation of PETRA and the continuing support given the Mark J Collaboration by the DESY Laboratory management. Conversations with the other PETRA experimental groups and the theory group have been indispensible. In particular we have profited from discussions with Dr. W. J. Marciano, Dr. W. Hollik, Professor F. A. Berends, Professor Paul Langacker, and Dr. B. Naroska. This work was supported in part by the U.S. Department of Energy under Contracts Nos. DE-AC02-76ER030609 and DE-AC02-76CH00016. S.A. and M.F.W. were supported by the Pakistan Atomic Energy Commission. The work at Physikalisches Institute, Technische Hochschule, D-5100, Aachen, Federal Republic of Germany was supported by the Deutsches Bundeministerium für Forschung und Technologie.

*Present address: University of California at San Diego, La Jolla, CA 92093.

†Present address: Institut für Hochenenergiephysik, Eidgenossische Technische Hochschule, CH-8093 Zurich, Switzerland.

‡Present address: University of Maryland, College Park, MD 20742.

§Present address: Laboratory for Nuclear Science, MIT, Cambridge, MA 02139.

**Present address: Boston University, Boston, MA 02215.

[1]S. L. Glashow, Nucl. Phys. **22**, 579 (1961); A. Salam, in *Elementary Particle Theory: Relativistic Groups and Analyticity (Nobel Symposium No. 8),* edited by N. Svartholm (Almqvist and Wiksell, Stockholm, 1968), p. 361; S. Weinberg, Phys. Rev. Lett. **19**, 1264 (1967); Phys. Rev. D **5**, 1412 (1972); S. L. Glashow, J. Iliopoulos, and L. Maiani, *ibid.* **2**, 1285 (1970).

[2]For the first such measurements, see JADE Collaboration, W. Bartel *et al.*, Phys. Lett. **108B**, 140 (1982); TASSO Collaboration, R. Brandelik *et al.*, *ibid.* **110B**, 173 (1982); Mark J Collaboration, B. Adeva *et al.*, Phys. Rev. Lett. **48**, 1701 (1982); Pluto Collaboration, Ch. Berger *et al.*, Z. Phys. C **21**, 53 (1983).

[3]A. Böhm, in *Pheomenology of Gauge Theories,* proceedings of the 1984 Rencontre de Moriond, La Plagne, France, 1984, edited by J. Tran Thanh Van (Editions Frontières, Gif-sur-Yvette, 1984), p. 209.

[4]F. A. Berends and R. Kleiss, Nucl. Phys. **B177**, 237 (1981); F. A. Berends *et al.*, *ibid.* **B202**, 63 (1982). For a review of radiative corrections and further references, see F. A. Berends and A. Böhm, in *High Energy Electron Positron Physics,* edited by A. Ali and P. Söding (World Scientific, Singapore, in press).

[5]M. Böhm and W. Hollik, Phys. Lett. **139B**, 213 (1984); R. J. Cashmore *et al.*, Z. Phys. C **30**, 125 (1986); B. W. Lynn and R. G. Stuart, Nucl. Phys. **B253**, 216 (1985).

[6]A. Sirlin, Phys. Rev. D **22**, 971 (1980); **29**, 89 (1984); W. J. Marciano and A. Sirlin, *ibid.* **29**, 945 (1984).

[7]Ugo Amaldi *et al.*, Phys. Rev. D **36**, 1385 (1987); F. Jegerlehner, Z. Phys. C **32**, 195 (1986).

[8]W. Hollik, in *Progress in Electroweak Interactions,* proceedings of the XXI Rencontre de Moriond, Les Arcs, France, 1986, edited by J. Tran Thanh Van (Editions Frontières, Gif-sur-Yvette, 1986), p. 3; M. Böhm *et al.*, Z. Phys. C **27**, 523 (1985); Fortschr. Phys. **34**, 687 (1986).

[9]B. Adeva *et al.*, Phys. Rep. **109**, 133 (1984); J. Mnich, Ph.D. thesis, Rheinisch-Westfälischen Technischen Hochschule Aachen, 1987.

[10]UA1 Collaboration, G. Arnison *et al.*, Phys. Lett. **166B**, 484 (1986); UA2 Collaboration, R. Ansari *et al.*, Phys. Lett. B **186**, 440 (1987); P. Jenni, in *Lepton and Photon Interactions,* proceedings of the International Symposium on Lepton and Photon Interactions at High Energies, Hamburg, West Germany, 1987, edited by R. Rueckl and W. Bartel [Nucl. Phys. B, Proc. Suppl. **3** (1987)].

[11]L. A. Ahrens *et al.*, Phys. Rev. Lett. **51**, 1514 (1983); **54**, 18 (1985); F. Bergsma *et al.*, Phys. Lett. **117B**, 272 (1982); **147B**, 481 (1984).

[12]Recent references concerning the data in Table III are CELLO Collaboration, H.-J. Behrend *et al.*, Phys. Lett. B **191**, 209 (1987); JADE Collaboration, B. Naroska, Phys. Rep. **148**, 68 (1986); Mark J Collaboration, J. Mnich, thesis, Rheinisch-Westfälischen Technischen Hochschule Aachen, 1987; PLUTO Collaboration, Ch. Berger *et al.*, Z. Phys. C **21**, 53 (1983); TASSO Collaboration, H.-U. Martyn, in *The Standard Model, The Supernova 1987A,* proceedings of the XXII Rencontre de Moriond, Les Arcs, France, 1987, edited by J. Tran Thanh Van (Editions Frontières, Gif-sur-Yvette, 1987), p. 63; HRS Collaboration, M. Derrick *et al.*, Phys. Rev. D **31**, 2352 (1985); MAC Collaboration, W. W. Ash *et al.*, Phys. Rev. Lett. **55**, 1831 (1985); Mark II Collaboration, M. E. Levi *et al.*, *ibid.* **51**, 1941 (1983); UA1 and UA2, see Ref. 8; Chicago-Columbia-Fermilab-Rochester-Rockefeller (CCFRR) Collaboration, P. G. Reutens *et al.*, Phys. Lett. **152B**, 404 (1985); CERN-Dortmund-Heidelberg-Saclay (CDHS) Collaboration, H. Abramowicz *et al.*, Phys. Rev. Lett. **57**, 298 (1986); CHARM Collaboration, J. V. Allaby *et al.*, Phys. Lett. B **177**, 446 (1986); Fermilab-MIT-Michigan (FMM) Collaboration, D. Bogert *et al.*, Phys. Rev. Lett. **55**, 1969 (1985); CHARM Collaboration, F. Bergsma *et al.*, Phys. Lett. **117B**, 272 (1982); **147B**, 481 (1984); BNL Experiment No. 734, L. A. Ahrens *et al.*, Phys. Rev. Lett. **51**, 1514 (1983); **54**, 18 (1985); G. Barbellini and C. Santoni, Riv. Nuovo Cimento **9**, 1 (1986).

[13]H. Fesefeldt, in *Proceedings of the XXXIII International Conference on High Energy Physics,* Berkeley, California, 1986, edited by S. C. Loken (World Scientific, Singapore, 1987), p. 970; H.-U. Martyn, in *The Standard Model, The Supernova 1987A* (Ref. 12); F. A. Berends and A. Böhm, in *High Energy Electron Positron Physics* (Ref. 4); J. Mnich, Ref. 9.

[14]Our last publication of τ leptons is B. Adeva *et al.*, Phys. Lett. B **179**, 177 (1986). The data were from an integrated luminosity of 115 pb^{-1}.

[15]For an exhaustive list of references of measurements of $R_{\tau\tau}$ and $A_{\tau\tau}$ see F. A. Berends and A. Böhm, in *High Energy Electron Positron Physics* (Ref. 4); and E. Deffur, Ph.D. thesis, Rheinisch-Westfälischen Technischen Hochschule Aachen, 1988.

[16]E. H. Thorndike, *Proceedings of the 1985 International Symposium on Lepton and Photon Interactions at High Energies,* Kyoto, Japan 1985, edited by M. Konuma and K. Takahashi (Research Institute for Fundamental Physics, Kyoto University, Kyoto, 1986), p. 407; B. C. Barish and R. Stroynowski, Phys. Rep. **157**, 1 (1988).

[17]JADE Collaboration, W. Bartel *et al.*, Z. Phys. C **24**, 223 (1984); CELLO Collaboration, H.-J. Behrend *et al.*, Phys. Lett. **158B**, 536 (1985); MAC Collaboration, W. T. Ford *et al.*, Phys. Rev. Lett. **51**, 257 (1983).

[18]B. Naroska, Phys. Rep. **148**, 68 (1987).

[19]B. Adeva *et al.*, Phys. Rep. **109**, 133 (1984); C. C. Zhang, DESY Report No. 85-073, 1985 (unpublished).

[20]F. A. Berends *et al.*, Nucl. Phys. **B253**, 421 (1985); **B253**, 441 (1985).

[21]See Ref. 11 for data at an average energy of $\sqrt{s} = 34.6$ GeV.

[22]S. M. Berman, J. D. Bjorken, and J. B. Kogut, Phys. Rev. D **4**, 3388 (1981).

[23]C. Carimalo *et al.*, Phys. Rev. D **20**, 1057 (1979); A. Courau, Phys. Rev. Lett. **49**, 963 (1982); Ch. Berger and J. H. Field, Nucl. Phys. **B168** 585 (1981).